

## TOPIC 3 – Procedures

### Field load tests on a Queen-post timber truss

Jorge M. Branco<sup>1,a</sup>, Paulo J.S. Cruz<sup>1,b</sup>, Maurizio Piazza<sup>2,c</sup> e Humberto Varum<sup>3,d</sup>

<sup>1</sup>ISISE, University of Minho, Campus de Azurém, 4800-058 Guimarães, Portugal

<sup>2</sup>DIMS, University of Trento, Via Mesiano 77, 38050 Trento, Italy

<sup>3</sup>DECivil, University of Aveiro, Campus Universitário de Santiago, 3810-193 Aveiro, Portugal

<sup>a</sup>jbranco@civil.uminho.pt, <sup>b</sup>pcruz@civil.uminho.pt, <sup>c</sup>mauriziopiazza@ing.unitn.it, <sup>d</sup>hvarum@ua.pt

**Keywords:** Timber truss, field tests, numeric analysis, semi-rigid joints

**Abstract.** In-situ cyclic tests on a Portuguese Queen-post timber truss were performed. The main goal of the tests was to evaluate the overall behaviour of the timber truss under symmetric and non-symmetric loading. Moreover, the influence of the number and location of point loads, without and with eccentricity relatively to joints, was assessed. The carrying tests were preceded by a visual inspection and non-destructive evaluation aiming to collect geometric data and to assess the decay level presented by the timber elements. The tests results have been reproduce through a finite element model assuming the moment-rotation laws proposed in previous research steps for the joints behaviour.

#### 1. Introduction

The lack of practical, but realistic, numerical models for the simulation of the behaviour of joints in traditional timber structures normally leads to the replacement of old roof structures, instead of their retrofitting to satisfy safety and serviceability requirements present in recent Codes and Recommendations. Moreover, the misunderstanding of the global behaviour of traditional timber roof structures can result in unacceptable stress distribution in the members, as a result of inappropriate joints strengthening, in terms of stiffness and/or strength [1]. To overcome this need, laboratory tests on scaled or full-scale specimens of members, connections and trusses can be done. However, only with field tests the structural global behaviour in real conditions can be evaluated.

Field tests on traditional timber trusses are not common. Researchers [2, 3 and 4] have preferred to transport the full-scale specimens to laboratory. In-situ working conditions are a barrier and the setup implementation (measurement system and load application) is often difficult.

The work presents the field test results of a Queen-post timber truss under symmetric and non-symmetric loading. The influence of the number and eccentricity (relatively to the joints) of point loads was studied. The truss has been characterized with regard to geometry, material properties and material decay using non-destructive tests. A numerical analysis based on the finite element method has been developed to reproduce the test results.

#### 2. Truss assessment

The Queen-post timber truss evaluated belongs to the roof structure of an old warehouse of Adico industry, located at Avanca (55 km South from Oporto). The exact date of the construction is not known but the industry exists since 1920 and some plans of the village from 1942 already show the warehouse. Trusses are the main elements of the roof structure, covered with ceramic tiles,

presenting a slope of  $27^\circ$  and rafters spaced 50 cm over the purlins and the ridge. The free span of the trusses is 11.8 m and the average distance between their centres is 3.5 m.

The geometry of the truss is particular: the configuration is typical of a King-post truss, but posts were added connecting joints struts-rafters with the tie beam. This is not the theoretical Queen-post truss geometry, in which the king post is substituted by a straining beam connecting horizontally (in the superior part) the two queen posts, those located below the higher purlin, and the struts connecting the bottom part of the queen posts to the lower purlins. Clearly, the truss evaluated it is an example of an incorrect truss configuration for the span of the roof. The correct Queen-post truss geometry should have been used or two extra posts (princess posts) should have been placed below the lower purlin. In fact, point loads out of the joints, increasing significantly the rafters bending moments, are the most common error detected in the preliminary survey performed in previous steps of the research program, see [5].

The truss is made of Maritime pine (*Pinus pinaster*, Ait.). The timber members of the truss are slender, as characteristic of traditional Portuguese roofs structures, with cross-sections varying from  $80 \times 145 \text{ mm}^2$  for the struts to  $80 \times 220 \text{ mm}^2$  for the tie beam. The tie beam is suspended from the posts by iron straps nailed to the posts. Between the tie beam and the king post there is a gap of 5 cm while queen posts are in contact with the tie beam. Connections between the others timber members are made by single step joints, in some cases nailed, and the queen posts-rafters connections have a heel strap nailed (25 mm wide and 5 mm tick), Fig. 1.

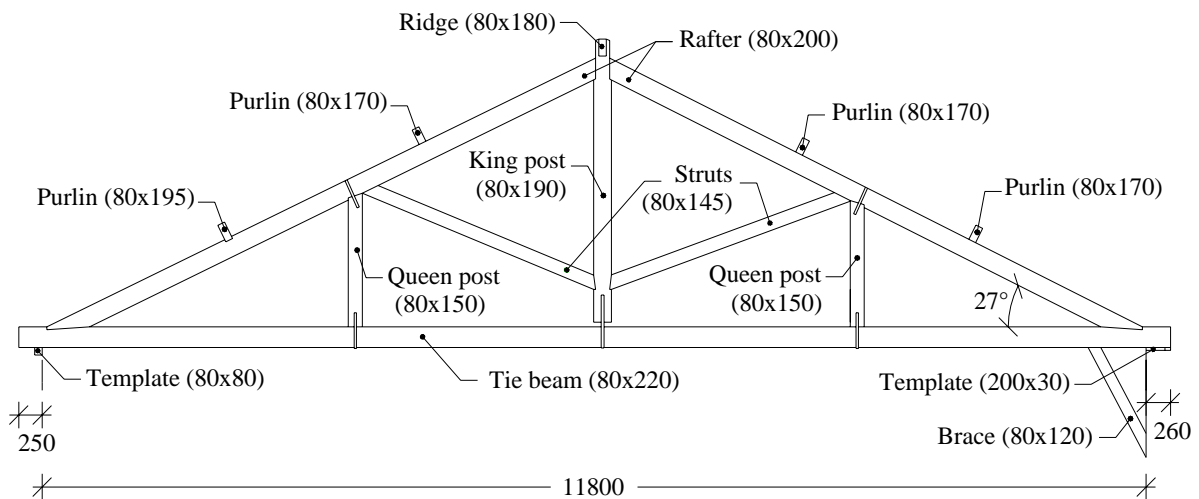


Figure 1: Adico Queen-post timber truss geometry (mm)

Despite the apparent good condition of the timber members of the truss, the visual inspection revealed insects attack in the tie beam, posts and struts. In these timber members, emergence holes over the surface of sapwood are visible however, without signs of active infestation.

To evaluate the extension of decay in the timber truss, Fig. 2, Pilodyn® and Resistograph® non-destructive tests were performed. The Pilodyn 6J allows to assess the surface hardness through the depth penetration of the pin steel (2.5 mm) measured in each test performed, while Resistograph was used to calculate the residual cross-section. Resistograph test permits to plot profiles (drill resistance *versus* penetration depth) that can be used to identify variation in material density and to determine the location and extent of voids, since decayed wood presents lower penetration resistance. The residual cross-section was defined by taking off the amount of wood decayed recognized through the Resistograph tests profiles, see Fig. 2.

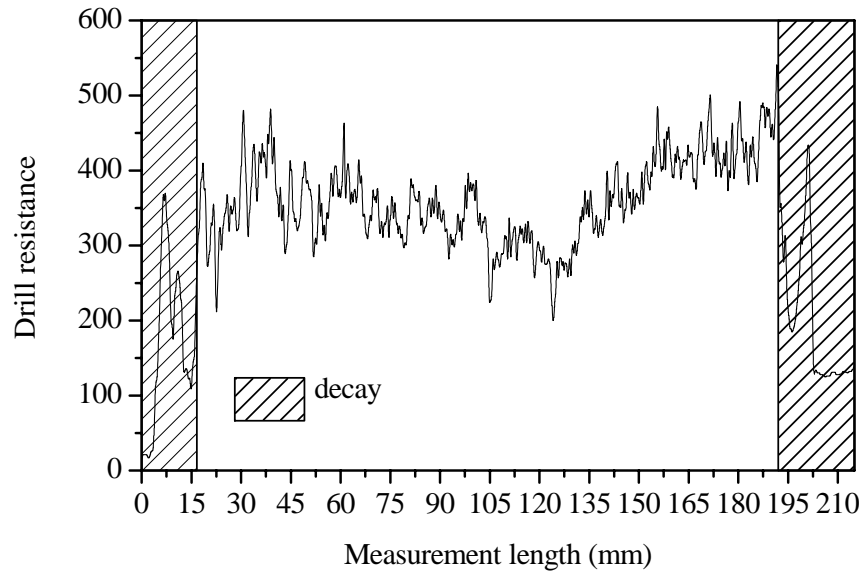


Figure 2: Calculation of the residual cross-section based in a Resistograph test profile

### 3. Test setup, instrumentation and procedure

The main goal of the tests was to evaluate the overall behaviour of the timber truss selected under symmetric and non-symmetric loading. Moreover, as consequence of the roof structure definition, the influence of the point loads number and location, without and with eccentricity relatively to joints, was assessed. Therefore, firstly, points loads were applied in the joints ( $F_1$ ,  $F_2$  and  $F_3$ ) and, in a second step, point loads were applied over the purlins and ridge ( $F_1$ ,  $F_4$ ,  $F_5$ ,  $F_6$  and  $F_7$ ).

Loading and unloading were recorded and an attempt to measure the creep of the structure under symmetric loading was made. The behaviour of the truss under non-symmetric loading was evaluated, in the first scheme (3 point loads), only by one test and in the second (5 point loads) with two tests (one in each pitch side). Table 1 resumes the field load-carrying tests performed.

Table 1: Summary of the field load-carrying tests performed

Procedure				Procedure			
Test	Point loads	Test	Point loads	Test	Point loads	Test	Point loads
3FC	$F_1$ , $F_2$ and $F_3$	3F-N	$F_3$	5FS	$F_1$ , $F_4$ , $F_5$ , $F_6$ and $F_7$	5FC	$F_1$ , $F_4$ , $F_5$ , $F_6$ and $F_7$
				5FN1	$F_6$ and $F_7$		
				5FN2	$F_4$ and $F_5$		

Wood pallets suspended from the truss by four steel cables ( $\phi$  6 mm) supported the 35 kg cement bags used as loads. Each loading and unloading procedure was divided in steps of 175 kg (5 bags). A total load of 2625 kg (3x875 kg) and 2975 kg (5x595 kg) was used in the first (three point loads)

and second (five point loads) schemes, respectively. The difference in the maximum load value applied between both schemes, 350 kg, is due to the difficulty to increase the number of bags over the pallets in the first case, while in the second scheme, the total number of available cement bags was used (85). To record the deformation of the truss during the tests, eight LVDTs (Linear Variable Differential Transformer) and six dial gauges (DG) were used. LVDTs were responsible for measuring the global displacement (LVDTs 1 to 3), the behaviour of the king post-tie beam connection (LVDT-5) and the displacement below the purlins (LVDTs 4 to 8) also used to calculate the rotational behaviour of rafter-tie beam and rafter-strut joints. The values of the LVDTs during the tests were acquired by a Data Acquisition System with 8 channels and using LabVIEW software package [6]. Dial gauges measured the opening of the queen post-tie beam connections (DG 3 and 4), the horizontal displacement of the rafter in the rafter-tie beam connections (DG 5 and 6) and two additional points to calculate the rotation of rafter-tie beam connections (DG 1 and 2). Fig. 3 shows the instrumentation used in the tests performed.

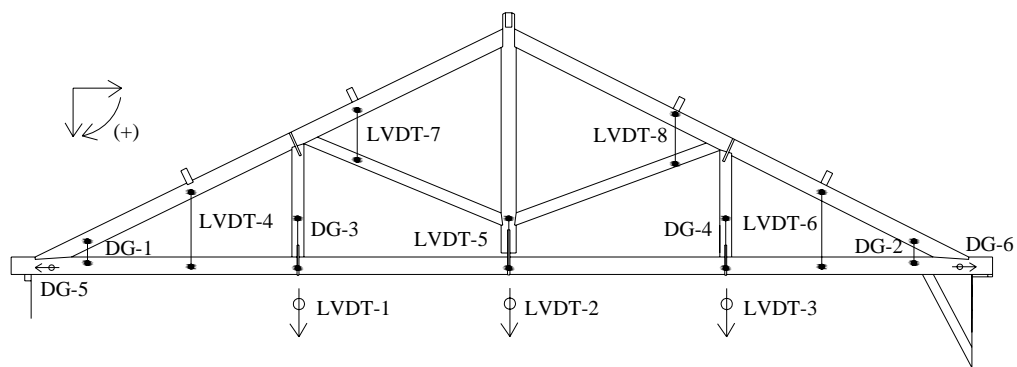


Figure 3: Instrumentation used in the tests. Eight LVDTs and six DGs

In every loading and unloading step, displacement values of the LVDTs were recorded; however, in the case of the dial gauges, only some steps were acquired, as results of the little variation verified.

#### 4. Analysis of the tests results

The behaviour of traditional timber trusses is highly depending on the variability of the material properties (wood is a natural and anisotropic material), member cross-sections (frequently, the changes in the trunk cross-section are reported along the members length), connections (because stresses are directly transferred by compression and/or friction between the surfaces in contact, the geometry and the level of detail are essential), supports (stiffness and location relatively to the rafter-tie beam joints) and loading conditions (point loads should be directly applied in the joints). Moreover, in the case of old constructions, due to decay processes and lack of maintenance, this heterogeneity is emphasized.

The field test results confirm that the truss under investigation presents a non-symmetric response even when subjected to symmetric loading conditions, Fig. 4.

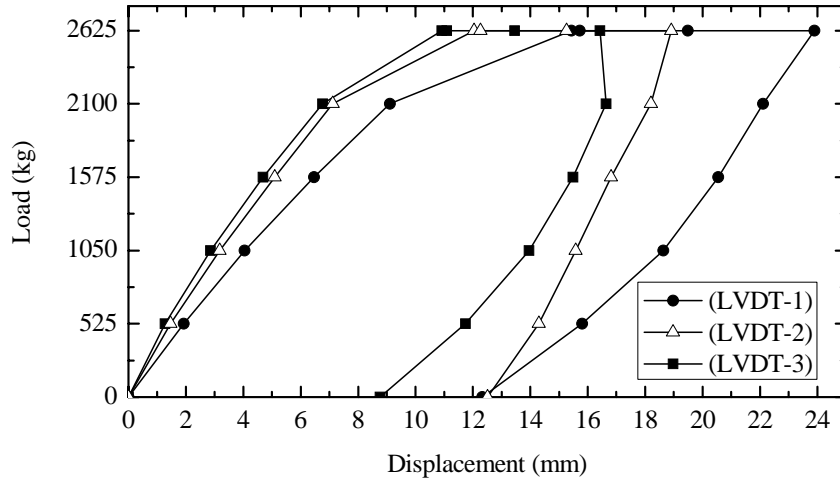


Figure 4: Displacement recorded by LVDTs 1, 2 and 3 during 3FC test

The difference observed between the load-displacement curves of LVDT's 1, 2 and 3 can represent the influence of the decay detected on the left queen post. The constant load value applied during 161 minutes in 3FC test (see Table 1) causes a significant increase of the truss deformations. The truss presents important plastic deformations (average value of 57%) after the complete unloading. The king post-tie beam connection works effectively, *i.e.*, the tie beam is suspended from the king post, see Fig. 5.

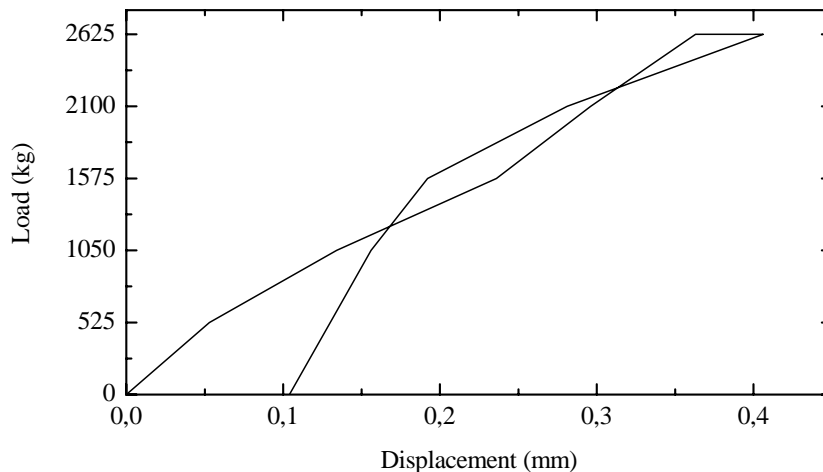


Figure 5: Behaviour of the king post-tie beam connection during 3FC test

The heel strap is able to suspend the tie beam, reducing therefore the deformation of this element (see LVDT-2 in Fig. 4). The connections between the queen posts and the tie beam, where a heel strap suspends the tie beam, show different behaviours (Fig. 6). Only the left connections, measured by DG-3, in the second series of tests (5 point loads – 5FS), behave properly - tie beam suspended from the queen post. In the first series of tests, both tie beam-queen post connections present residual deformations as a clear indication that, before tests, those connections were dismantled. The first series of tests were sufficient for the left connections to recover, while the gap between both connected elements existing in the right connection was never recovered (recorded by DG-4).

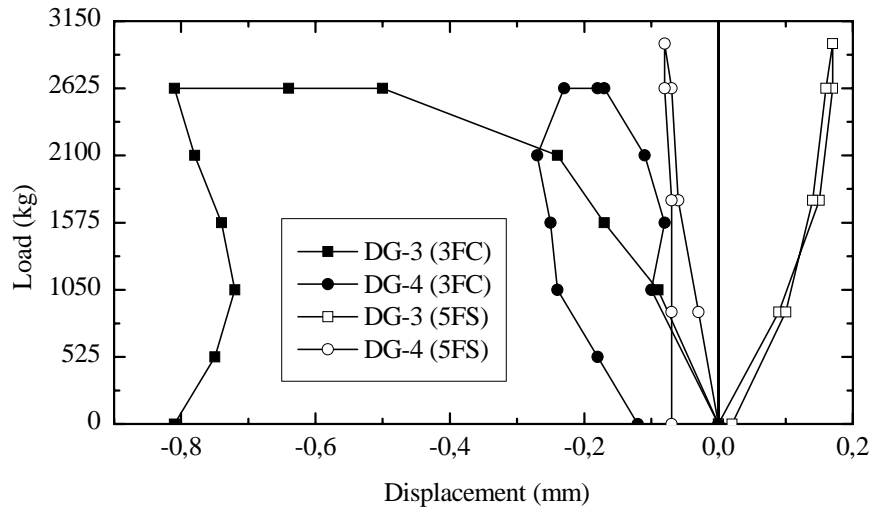
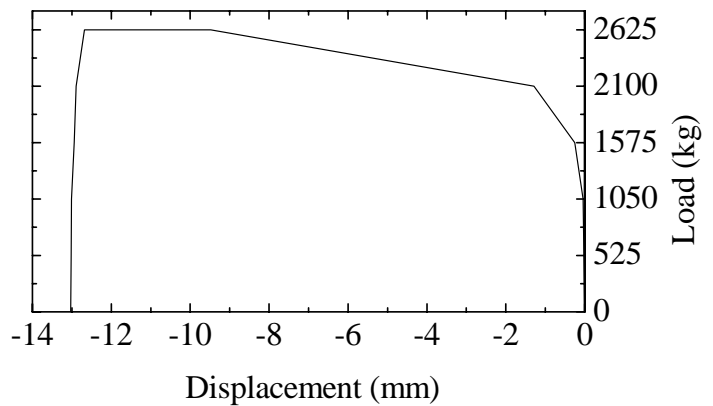


Figure 6: Behaviour of tie beam-queen post connections during 3FC and 5FS tests. Negative values are recorded when the two connected elements are approaching

During 3FC test, significant damage was detected on the left rafter-tie beam connection, over the DG-5 (Fig. 7a). Damage started for a load level of 2100 kg and, when 2550 kg were reached, DG-5 measurements were unstable (increasing with a constant rate) during 30 minutes. At the end of the loading period, the maximum relative horizontal displacement between the rafter and the tie beam (measured by DG-5) was reached and no recover was observed during and after the unloading procedure (Fig. 7b).



a) Damage



b) Load-displacement curve of DG-5

Figure 7: Behaviour of the left rafter-tie beam connection during 3FC test

Under non-symmetric loading, as the one imposed during 3FN test, distortion of the truss is observed, in particular, in the tie beam, as shown in Fig. 8. Non-symmetric behaviour is acquired by LVDT-1 and 3 with lower values in the first LVDT as consequence of the bigger stiffness (compression of the left queen post).

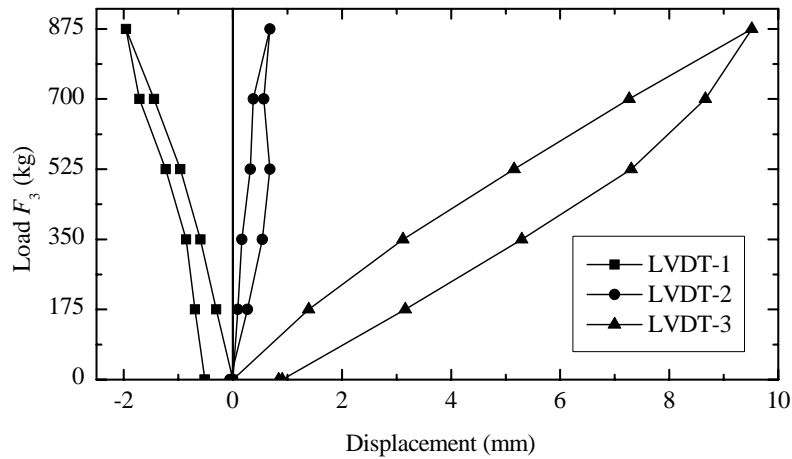


Figure 8: Displacement recorded by LVDTs 1, 2 and 3 during 3FN test

Dividing the total amount of load applied by more point loads in the second tests series, from 3 to 5, the same general conclusions about the asymmetric behaviour of the truss, even when subjected to symmetric loading, can be drawn. The main difference between the tests under 3 and 5 point loads is, in the second case, the introduction of significant bending stresses in the rafters. In the second series of tests, greater values of rotation in the connections are obtained (Fig. 9) while the global displacements are lower (Fig. 10), when compared with the 3 point loads case. In the first case, the system is more rigid.

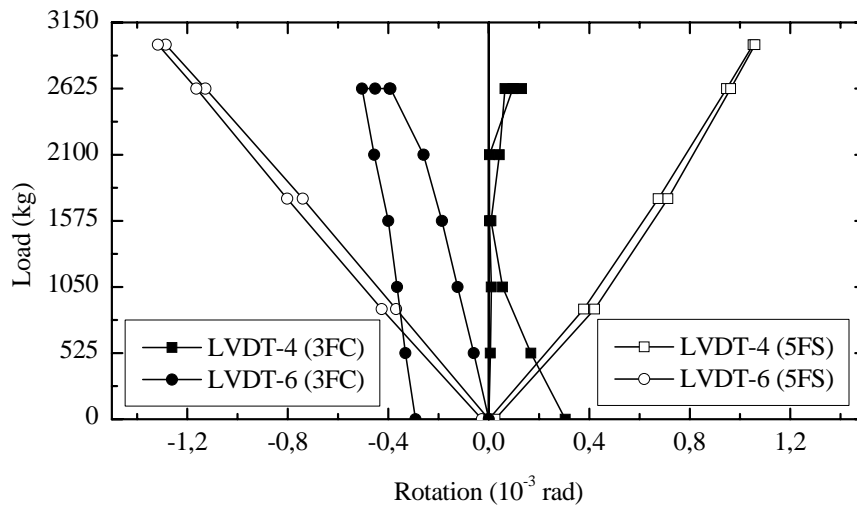


Figure 9: Comparison between rotations calculated based on values recorded by LVDTs 4 and 6 during 3FC and 5FS tests

Applying the point loads with eccentricity relatively to joints, the main stresses are found in the rafters, caused by bending, and greater rotations of the rafter-struts and rafter-tie beam connections are obtained. When the point loads are applied directly in the joints, the main stresses are observed in queen posts (compression), pushing the tie beam down. As a consequence, LVDTs 1, 2 and 3 show higher values of displacement (see Fig. 10). In addition, the creep behaviour observed during 3FC test is significantly greater but, in this case, the influence of the damages observed in the rafter-tie beam connection must be taken into account.

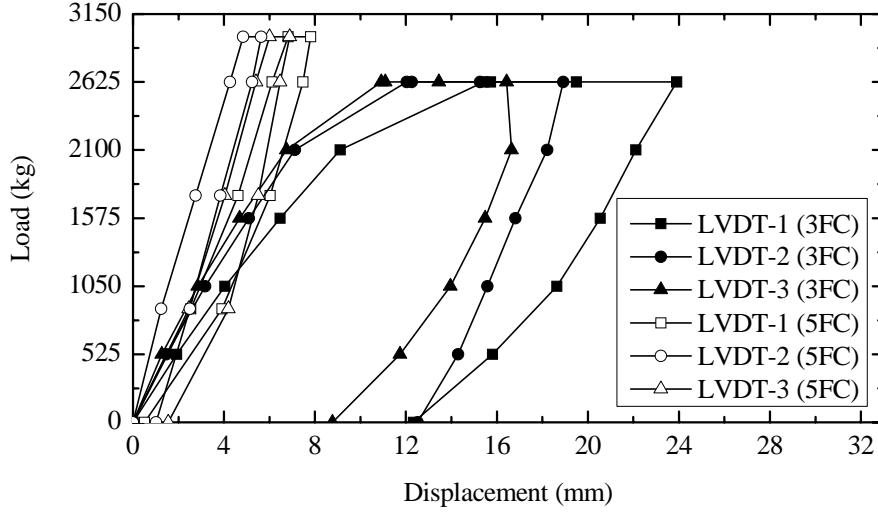


Figure 10: Comparison between the displacements recorded by LVDTs 1, 2 and 3 during 3FC and 5FC tests

## 5. Numeric analysis

The structural analysis program SAP2000 [7] has been used to model the field tests carried out. It has been developed a model involving variable dimensions beam elements, assuming the material properties suggested by [8] for the Maritime pine wood (*Pinus pinaster*, Ait.), connected through semi-rigid joints modelled using nonlinear link elements (Nlinks). The Nlinks elements, used in all connections between timber structural elements of the truss, placed in the end of the connected elements with a negligible length, are characterized by axial stiffness (see Eq. 1) and rotational stiffness defined by means of a Moment-Rotation law (see Fig. 12). The conclusion of the preliminary inspection and evaluation phase carried out were introduce in the model, in particular, cross-sections have been reduced according to the map of decay (see Fig. 2).

$$k_{ax} = \frac{E_{\alpha} \times S}{l} \quad (1)$$

where, applying the Hankinson Equation (Eq. 2):

$$E_{\alpha} = \frac{E_0}{\cos^2 \alpha + \frac{E_0}{E_{90}} \sin^2 \alpha} \quad (2)$$

represents the wood elastic modulus in the direction forming an angle  $\alpha$  with the fiber.

$$l = \frac{h}{2 \sin \alpha} \quad (3)$$

represents the nominal notch length, where compression deformation occurred.

$$S = \frac{A_{rafter}}{\sin \alpha} \quad (4)$$

represents the nominal notch area, where stress was assumed to be transmitted.

The axial stiffness of tie beam-queen posts connections ( $k_{ax,hs}$ ) has been formulated taking into account the axial stiffness of the heel strap:

$$k_{ax,hs} = \frac{E_{steel} \times A_{heel\ strap}}{l_{heel\ strap}} \quad (5)$$

where  $E_{steel}$  is modulus of elasticity of steel,  $A_{heel\ strap}$  and  $l_{heel\ strap}$  is the cross-section and the length of the heel strap, respectively.

Bilinear moment-rotation laws directly derived from [9] were assumed for the Nlinks elements responsible to model the semi-rigid behaviour of the connections. Fig. 11 highlights the behaviour of the connections at first loading. The first branch, for moments inferior then  $M_y^+$  or  $M_y^-$ , is elastic, for positive rotation and negative rotation, are characterised, respectively, by a slope  $k_e^+$  or  $k_e^-$ . For increasing moment beyond the elastic limit, the connection responds following a second lines branch, with the slope  $k_p^+$  or  $k_p^-$ , for positive or negative rotations.

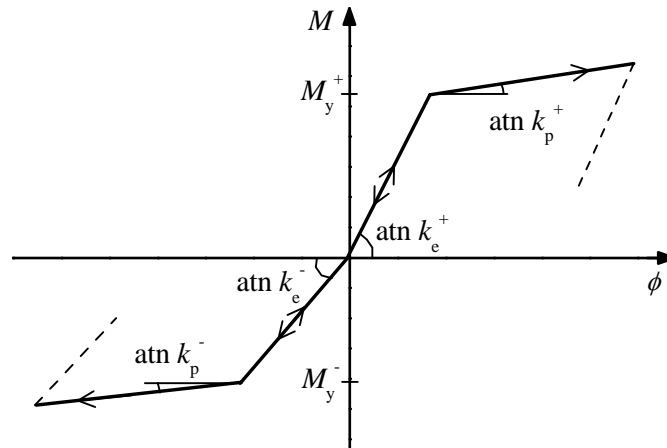


Figure 11: Bilinear moment rotation laws adopted in the numerical modelling of the non-symmetric tests

## 5.1. Numeric versus tests results

Numerical modelling and experimental results have been compared. First, *Step 0*, the numeric model has been implemented without considering the real behaviour of the truss observed in the performed tests. Then, *Step 1*, the model was verified and calibrate based in the tests results. Symmetric tests were used essentially to calibrated the axial stiffness of the connections while rotational stiffness have been adjusted with asymmetric tests results. In the following the main conclusions of the model efficiency are discussed and presented.

### 5.1.1. Symmetric loading tests

Using the calculate connections axial stiffness obtained from Eq. 1, *Step 0*, the computed values for the global displacements (LVDT 1 to 3) represents only 33% of the test results obtained for the first test (3FC). The main reason for this difference is the fact that all connections, in particular the ones between the posts and the tie beam, showed significant gaps between the metal devices and the joint itself. Moreover, the deterioration and loss of strength of the steel elements are not considered in the calculated stiffness values. The gaps between the metal devices and the joints are confirmed by the tests results (see Figs. 5 and 6). It is also important to point out that the plastic deformation measured in the global displacement after the 3FC test represents 52%, 66% and 53% of the maximum displacement, respectively for LVDT 1, 2 and 3. In the case of the relative displacements measured in the tie beam-posts connections, the residual values represents 57%, 100% and 52% of the maximum displacement recorded through LVDT-5, DG-3 and DG-4, respectively. Therefore, the stiffness values calibrated for the first test performed, 3FC, should only be account as informative because they report the influence of the original gaps existing between the metal devices and the joints. It is important to note that during the 3FC test a significant damage of the

left rafter-tie beam connection was detected (Fig. 7a) which influences directly the global displacements values. However, the calibrated model was able to reproduce the non-symmetric response of the truss even under symmetric loading conditions applied during the 3FC test (Fig. 12).

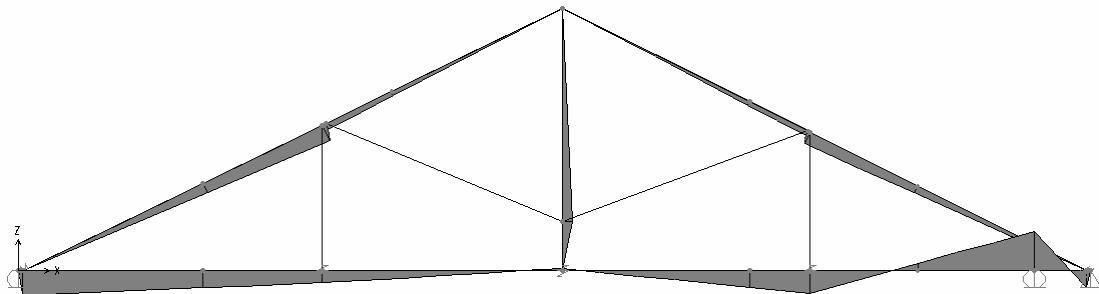


Figure 12: Bending moment on the truss caused by 3FC test

Table 2 gives a comparison between experimental and numeric results for both symmetric loading tests performed, with regard to the displacements in the relevant joints of the truss. The values reported in Table 2 are the maximum displacement of the symmetric loading tests performed. Table 2 shows a good fit between the values worked out by means of the numeric model and the tests results, with exception of LVDTs 2 and 3 values, all errors reported by the numeric model are under 10%. Experimental results for the global vertical displacement of the truss under the king post are clearly increase by the model. This inconsistency can be explained by the faulty connections between the king post and the tie beam. The heel strap must introduce a frictional stiffness which reduces the mid-span deformations of the tie beam when the truss is loaded. Ideally, in tie beam-post connections it shall be used a heel strap, nailed only in the post, suspending the tie beam with a connection without bending stiffness.

Table 2: Comparison between numeric modelling values (Num.) and tests results (Exp.).  
Displacement values in (mm) and Error express in (%)

Test 3FC											
LVDT-1			LVDT-2			LVDT-3			DG-3		
Exp.	Num.	Error	Exp.	Num.	Error	Exp.	Num.	Error	Exp.	Num.	Error
15,40	15,25	1,0	12,00	13,71	14,3	10,90	9,64	11,6	-0,64	-0,69	-7,8
LVDT-5			DG-4			DG-5			DG-6		
Exp.	Num.	Error	Exp.	Num.	Error	Exp.	Num.	Error	Exp.	Num.	Error
0,36	0,35	2,8	-0,18	-0,17	5,6	-0,25	-0,26	4,0	0,18	0,19	5,6
Test 5FS											
LVDT-1			LVDT-2			LVDT-3			DG-3		
Exp.	Num.	Error	Exp.	Num.	Error	Exp.	Num.	Error	Exp.	Num.	Error
7,53	7,98	6,0	4,48	4,94	10,3	5,30	5,40	1,9	-0,17	-0,18	5,9
LVDT-5			DG-4			DG-5			DG-6		
Exp.	Num.	Error	Exp.	Num.	Error	Exp.	Num.	Error	Exp.	Num.	Error
0,14	0,14	0,0	0,07	0,07	0,0	-0,28	-0,30	7,1	0,11	0,10	9,1

The calibration process of the numeric model shows that during the experimental campaign a stiffness updating of the connections occurs (see Table 3). This conclusion, confirmed by the test results (see Fig. 10), is due essentially to the fact that connections were originally dismantled (significant gaps existed between the metal devices and the joints). When using the numeric models, calibrated for the case of symmetric loading tests, under non-symmetric loading conditions, a significant discrepancy is obtained between the numeric and experimental results. In particular, the global displacement, LVDT-1, 2 and 3, and the connections between the tie beam and the posts, recorded by DG-3, DG-4 and LVDT-5 are sensible to the connections rotational stiffness.

Table 3: Axial stiffness values (kN/m) used in the numeric modelling

Test	DG-5	DG-6	DG-3	DG-4	LVDT-5
3FC	3900	10000	4000	3400	12000
5FS	292108	250169	4000	7000	30000

### 5.1.2. Non-symmetric loading tests

After the calibration of the connections axial stiffness based on the test results achieved through the symmetric loading tests, non-symmetric loading tests were used to assess the influence of the rotational connection's stiffness in the overall behaviour of the truss, in particular, under non-symmetric loading conditions. In this process, the chronology of the tests was considered, assuming the axial stiffness values as the ones calibrated with the model corresponding to the previous symmetric loading test. Therefore, in the model concerning the 3FN test, the axial stiffness assumed for the connections were derived from 3FC test and, the values assumed in the models of 5FN1 and 5FN2 tests, were based on the axial stiffness values calibrated through the numeric model of 5FS test. However, during the calibration process of the numeric model for the 3FS test case, it was necessary to update some connections axial stiffness. That fact allows to concluded that, after 3FC test, the response of the connections were still unstable, still depending of the gaps existing between the connected surfaces, like the calibration process of the axial stiffness of the connections have shown (see Table 3).

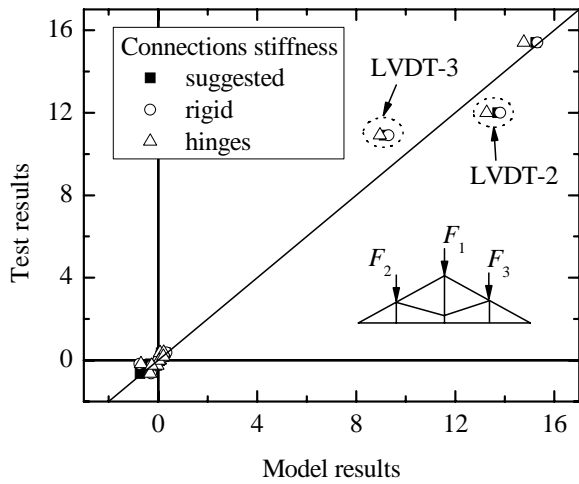
During the test history performed, the gaps of the connections were reduced and the axial stiffness of the connections increased. Table 4 shows the axial stiffness values updated during the calibration process of the model corresponding to 3FN test.

Table 4: Axial stiffness values (kN/m) used in the numeric model of 3FN test

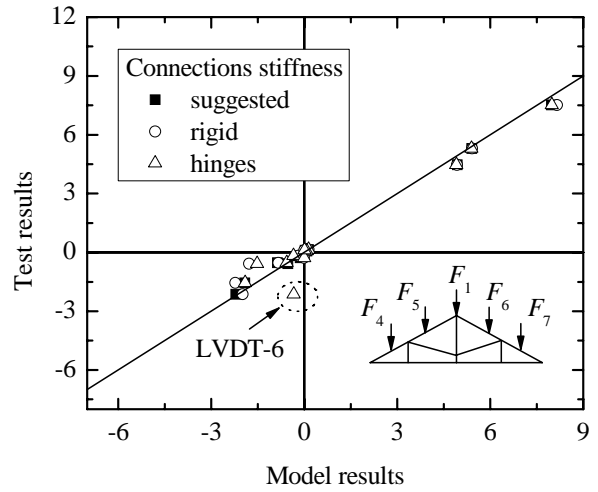
Test	DG-5	DG-6	DG-3	DG-4	LVDT-5
3FN	292108	17000	4000	7000	16000

Numerical modelling values have been compared with the tests results and a sensitivity study of the connections rotational stiffness value was performed. Therefore, in addition to the moment-rotation laws suggested by [9], the two extremes rotational stiffness models, rigid joints and perfect hinges, were evaluated. As expected, the connections rotational stiffness can be important under non-symmetric loading conditions and negligible for symmetric loading conditions. The numeric results (Fig. 13) shows that the influence of the rotational stiffness assumed for the connections under symmetric loading conditions (3FC and 5FS tests) is trivial.

The rotational stiffness assumed for the connections can change the deformation of the truss but, those variations are not important. The same is not true for tests under non-symmetric loading conditions. Fig. 14 shows that the rotational stiffness assumed for the connections as direct consequences in the truss overall behaviour under non-symmetric loading tests.

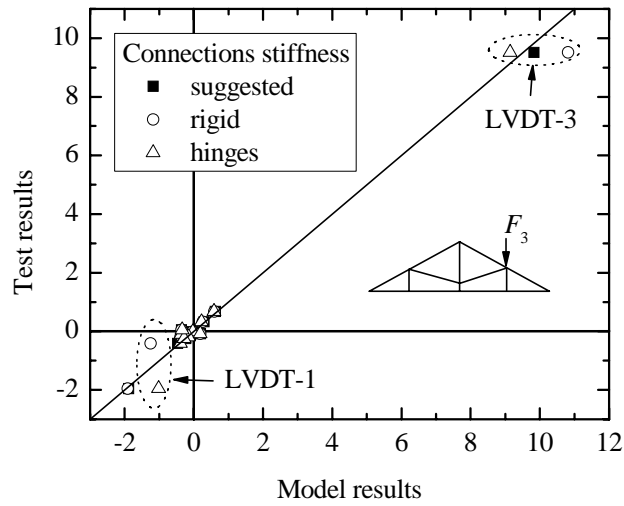


a) 3FC test

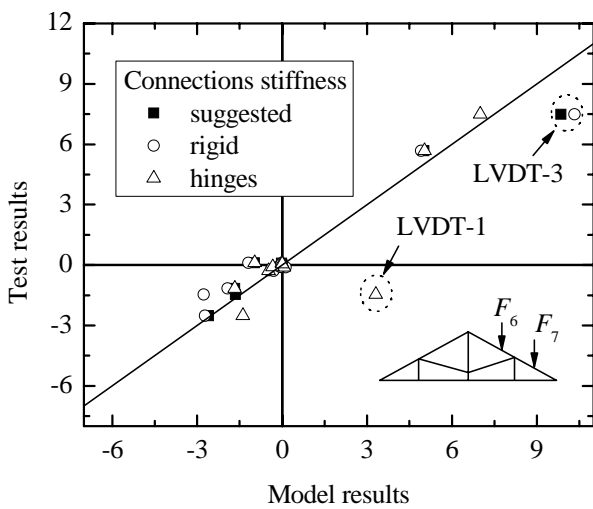


b) 5FS

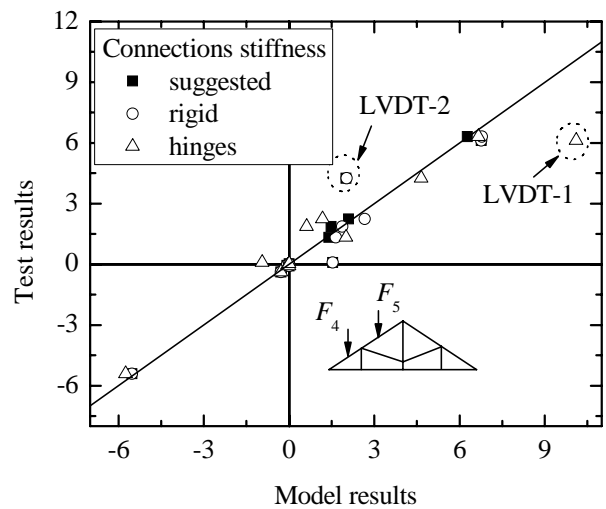
Figure 13: Rotational stiffness of connections influence in the model results in comparison with test results under symmetric



a) 3FN test



b) 5FN1 test



c) 5FN2 test

Figure 14: Rotational stiffness of connections influence in the model results in comparison with test results under non-symmetric loading

## 6. Conclusions

The work results highlight the importance of the *in-situ* experimentation, to assess the global behaviour of traditional timber trusses, identify the critical areas, to plan the upgrade interventions and to quantify their effects. Experimentation gave an insight of the truss behaviour hardly reachable otherwise. The effects of the incorrect truss configuration for the roof span, the faulty connections geometry and the existing gaps in the joints in the overall behaviour of the truss tested were assessed.

The numeric model implemented through a general purpose and very simple FE code [7], has proved to be an effective and accurate method of modeling timber truss behaviour, on condition that a semi-rigid behaviour of the traditional connections is assumed. The comparison between the tests results and the ones achieved by the numerical models shows that the rotational stiffness assumed for the connections has particular importance for the truss behaviour in terms of deformations under non-symmetric loading conditions, and the magnitude raise with the distortion introduced into the truss.

## Acknowledgments

Authors would like to acknowledge the cooperation of Adico industry (Arch. Luis Dias and Fernando) and José Manuel in the experimental campaign. The research described in this paper was conducted with financial support of the Portuguese Foundation for Science and Technology (POCI/ECM/56552/2004).

## References

- [1] M. Parisi and M. Piazza: Mechanics of plain and retrofitted traditional timber connections. *Journal of Structural Engineering*. 126(12): 1395-1403.
- [2] M. Del Senno and M. Piazza: Behaviour and rehabilitation of Queen-post timber trusses. A case study. In *STREMAH 2003: Structural Studies, Repairs and Maintenance of Heritage Architecture VIII*, May, Halkidiki, Greece.
- [3] M. Piazza, G. Brentari and M. Riggio: Strengthening and control methods for old timber trusses: the Queen-post truss of the Trento theatre. In *SAHC 2004: Structural Analysis of Historical Constructions*, Padova, IT, II: 957-965.
- [4] J.M. Branco, P.J.S. Cruz and M. Piazza: Diagnosis and analysis of two King-post trusses. In *SAHC 2008: Structural Analysis of Historical Constructions*, Bath, UK, 02-04 July.
- [5] J.M. Branco, P.J.S. Cruz, M. Piazza and H. Varum: Portuguese traditional timber roof structures, In *WCTE 2006 - World Conference on Timber Engineering*, 6-10 August, Portland, Oregon, USA.
- [6] LabVIEW: LabVIEW User's manual. Version 8.2. *National Instruments*.
- [7] SAP 2000. Static and dynamic finite element analysis of structures. Structural analysis program. User's manual. *Computers and Structures Inc.*, Advanced 10. California. USA.
- [8] LNEC: Timber for structures – Maritime pine for structures. LNEC (eds), 1997, *Ficha M2*. ISSN 0873-6472, Lisbon, 12 p. (only available in Portuguese).
- [9] J.M. Branco: Influence of the joints stiffness in the monotonic and cyclic behaviour of traditional timber trusses. Assessment of the efficacy of different strengthening techniques. PhD Thesis (Bi-Nationally). University of Minho and University of Trento, 2008.